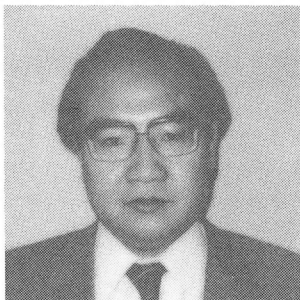
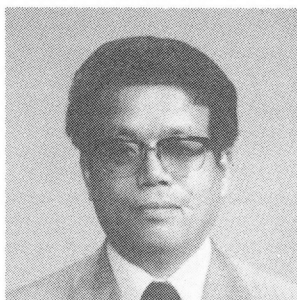


STRENGTH AND DEFORMATIONAL CHARACTERISTICS OF REINFORCED CONCRETE
SHELL ELEMENTS SUBJECTED TO IN-PLANE FORCES

(Translated from Transactions of JSCE.No.331, March, 1983)



Yukio AOYAGI



Kazuie YAMADA

SYNOPSIS

It is of importance to grasp the stress-strain behaviors of reinforcements and concrete and to reflect them properly in the sectional design of reinforced concrete (RC) shell elements subjected to in-plane forces. Although a number of theoretical researches have so far been conducted, very few experimental data are available to substantiate the validity of proposed theories. With the situation in mind an experimental study was carried out, in which 25 models of orthogonally reinforced concrete shell plate elements were loaded by in-plane forces biased to the directions of reinforcements, simulating the boundary conditions prevailing in the actual structures. Based on the experimentally obtained evidence that the direction of cracks and the average shear rigidity across cracks are dependent on ratios of orthogonal principal stresses and on crack widths, respectively, a simplified analytical procedure, by which the accuracy of estimation could be also improved, is presented.

Y. Aoyagi is a member of Japan Society of Civil Engineers, Japan Concrete institute, ACI, etc. and is the head of material mechanics section at Civil Engineering Laboratory, Central Research Institute of Electric Power Industry, Chiba, Japan. He received his MS in 1964 and his Doctor of Engineering Degree in 1974 from the University of Tokyo, Japan. His research interests include design and construction of concrete containments for nuclear reactors, in-ground tanks for storage of LNG, prediction of cracking and deformational behaviors of reinforced concrete members under extremely low and elevated temperatures, creep, shrinkage and thermal effects on concrete structures, etc. He is a member of ACI and has published several papers on the J Division of the proceedings of SMiRT Conferences.

K. Yamada is a member of JSCE, JCI, etc. and the chief of the section in charge of

concrete engineering for Technical Research Institute of Maeda Construction Company, Nerima, Tokyo, Japan. He graduated from Waseda University in 1964 and received his Doctor of Engineering Degree from the University of Tokyo for his study related to the present paper in 1981. His research interests include the design and construction of reinforced concrete containments, mass concrete, creep and shrinkage, etc.

1. PREFACE

Reactor containment vessels have been made of steel so far, but since the adoption of a prestressed concrete containment vessel was decided in the Tsuruga No. 2 reactor of Japan Atomic Power Co., the construction of the containment vessels made of prestressed concrete (PC) and reinforced concrete (RC) has begun to be studied extensively in the electric power companies concerned. However, in Japan, there was not available the standard to be used as the criteria for the design and construction of the concrete structures of this kind, and this fact has been a large obstacle at the time of their practical use. Accordingly, in the Ministry of International Trade and Industry, the Technical Standard Study Committee was established in 1977 for the purpose of drawing up the technical standard, and the draft was formed in November, 1979.

In the course of drawing up this technical standard, the provisions in various foreign countries such as ASME Sec.III, Div. 2 and German standard were referred to, but the base of the provisions concerning the aseismatic design of concrete containment vessels was not distinct, therefore the necessity of the research of Japan proper was pointed out. Thereupon, the experiments on a cylindrical scale model, a model of junction between cylindrical wall and foundation plate, push-off shearing test of a RC block, the test on a shell element and so on have been planned and carried out.

In the framework of this particular paper, as part of the research to confirm the technical standard described above, for the purpose of elucidating the strength and deformation characteristics when a RC containment vessel was subjected to earthquake force only, or to the combination of internal pressure and earthquake force, examination was carried out on the result of the test on RC shell elements subjected to uni-axial or bi-axial in-plane forces, and a proposal on the method of estimating the strength and deformation characteristics of a RC shell element was made. The range treated in this report was limited to the case of orthogonal bar arrangement, and in addition, to that the strength of a shell element was determined by the yield of reinforcing bars.

2. PAST RESEARCH CONCERNING THE MECHANICAL PROPERTIES OF RC SHELL ELEMENTS SUBJECTED TO IN-PLANE FORCES

When the RC shell elements with orthogonal bar arrangement are subjected simultaneously to in-plane membrane force and shearing force, the problem can be treated by substituting with the principal stresses acting in two directions making a certain angle with the directions of reinforcing bars. Namely, the problem of in-plane forces on RC shell elements can be reduced to the elucidation of the mechanical properties under the principal stresses acting with the declination α to reinforcing bars. The problem of this kind had become the object of research mainly in Germany as the problem of "Scheibe", and the equation of Leitz¹⁾ published in 1930 and the equation of Flügge²⁾ published in 1934 have been well known.

Thereafter until recent years, the development has been made centering around the analytical theory, and it may be said that the equation of Peter³⁾ published in 1966 and the equation of Baumann^{4),5)} and Duchon⁶⁾ published in 1972 were theoretically well systematized. Also, as the recently proposed equation, there is the equation of Bazant and Tsubaki⁷⁾ published in 1979, and friction theory was introduced into this by paying attention to the phenomenon that the width of cracks increase due to the unevenness of a cracked surface. The details of these

proposed equations were omitted on account of limited space, but respective proposed equations are shown in Table 1. These proposed equations were the results of theoretical research except that of Peter, and most of the analytical results have not been proved by experimental evidences. Accordingly, considering the above mentioned present status, the authors thought that after grasping the mechanical properties of RC shell elements by the model test simulating the stress condition working on them, it is necessary, to establish the practical analysis method of closely related to actual phenomena, and carried out the experimental research described hereinafter.

3. METHOD OF LOADING FOR RC SHELL ELEMENTS SUBJECTED TO IN PLANE FORCES

(1) Materials and Test Specimens

(a) Concrete and Reinforcing Bars

The mix proportion of the concrete used for the experiment is shown in Table 2. The yield point of the D 10 reinforcing bars used as the main reinforcing bars was 3780 kg/cm^2 (370MPa), and the tensile strength was 5510 kg/cm^2 (540MPa).

(b) Shape and Dimensions of Test Specimens

The shape and dimensions of the test specimens are shown in Figure 1. The central part of 10cm thickness of this test specimen (150cm x 150cm x 10cm) is designated as the part for obtaining test data. In order to make the anchoring of main reinforcing bars outside the region, the tapered part and the load-introducing region of 20cm thickness were attached on the peripheral part, therefore the total plane dimensions of the test specimen was 250cm x 250cm. The slits of 2cm width were provided on the peripheral part (see photos. 1,2 and 3) so that the required load was to act on the test part. The reinforcing bars were arranged in two orthogonal directions, in two layers in each direction. The grid spacing between the centers of reinforcing bars were 20cm in the test specimens No.1 ~ No.21, and 12.5cm in No.22 ~ No.27. However, only in the case of No.24 test specimen, the spacing of X-direction reinforcement were 12.5cm, and that of Y-direction reinforcement were 20cm.

Moreover, in the surroundings of bolt holes in the peripheral region and the boundary part between the test region and the peripheral region, sufficient reinforcing bars were arranged so that the failure in these parts did not precede.

(c) Construction and Curing of Test Specimens

Reinforcing bars were worked into the required shapes and dimensions, and thereafter, they were assembled in steel forms and placed horizontally in two orthogonal directions, in two upper and lower positions, so as to be covered by 2cm thick concrete. The covering was secured exactly with spacers, and the reinforcing bars were fixed by tying the intersecting places with wires. Also, in order to prevent the rapid opening of cracks generated in the slit parts, the reinforcing bars of D 6mm were arranged in two layers around the test part.

Concrete was mixed with a tilting mixer in the laboratory, and placed in the forms in which the arrangement of reinforcement had been completed. The concrete surface was finished with a trowel 3~4 hours after the placing, to prevent the plastic sinking and cracking of concrete. After removing the forms, curing was

performed with wet cloths over all surfaces of the specimens.

(d) Method of Introducing Initial Artificial Cracking

In the cases of some specimens, cracking was introduced into a part of the test specimens in predetermined direction at prescribed spacing prior to loading. The method of introducing cracking was to bond a plastic rod with equilateral triangle cross section of 5mm side onto the predetermined position in the form before concrete was placed, take it out before the test, and crack by pressing a hardened steel wedge into the groove formed on concrete surface.

The confirmation of cracking was made when the strain gauge pasted on a reinforcing bar at the position of crack generation showed 500μ , and the crack width was measured with a contact type strain meter.

(2) Loading of Test Specimens and Method of Measurement

(a) Outline of Loading Method

Since it was necessary to perform the test so that the test specimens were subjected to only membrane and in-plane shearing force, and the effect of bending moment should be eliminated as far as possible, a specially made suspending device using springs was employed, and by hanging at such position that bending moment was not generated at the middle of the test specimens due to their own weight, horizontal loading was applied.

i) Method of loading of uni-axial or bi-axial tension

The loading of in-plane tension was performed by so-called tournament system as shown in Figure-1 so that the load applied with one 100t oil hydraulic jack acted equally on four parts divided by the slits on the periphery of the test specimens. Each jack was arranged on both sides to pull from both sides.

In the case of bi-axial tension, two bob weights were attached over the diagonals of the test specimens, and four jacks were operated by adjusting them so that the position of the test specimens did not change during the test.

ii) Method of loading of compressive force

The loading of compressive force on the test specimens was carried out as shown in Figure-1 by the self anchoring type loading method composed of PC rods and four 50t oil hydraulic jacks.

iii) Procedure of loading

When cracking had not been introduced beforehand into the test specimens, the load up to respective phases of the initiation of cracking, the allowable stress and the yield of reinforcing bars was given, thereafter the load was removed, and loading was made again. When cracking had been introduced in the test specimens, the loading cycle up to the generation of cracks was omitted, and the loading up to the allowable stress of reinforcing bars was performed as the first cycle. In both cases, in the last cycle, load was applied until the test

specimens broke after the maximum strength was exceeded. In the case of two-direction loading, so-called proportional loading was performed, in which the ratio of the loads in both directions ($N_2/N_1=k$) was maintained always during the loading test.

(b) Items of Measurement and Method of Measurement

In this experiment, the cracking of RC slabs, the yield of reinforcing bars, ultimate strength, deformation property, the state of crack generation and the strain of reinforcing bars were taken as the main items of measurement. The 100t load cells made by T Co. attached to respective jacks were used, and load was measured with strain meters, 60 AB type made by K Co..

As for the strain of reinforcing bars, foil gauges (made by T Co., gauge length 2mm, resistance 120 Ω) were used, two gauges were stuck symmetrically at one point, and the mean value of two gauges was adopted as the strain at that point. The measured values were recorded with a multi-channel digital strain meter made by T Co. in order to determine the strain of reinforcing bars on a cracked surface, a typical reinforcing bar was selected, and strain gauges were stuck at intervals of 10cm over the whole length. The positions of measurement were somewhat different according to respective test specimens, but the vicinity of central part of the test specimens were measured extensively.

The measurement of the deformation of RC slabs was performed with a sliding type displacement gauge (made by T Co., 1/500mm accuracy) or a contact strain gauge, of which the gauge length was fixed at 10cm.

In the measurement of relative slip and opening on a cracked surface, a sliding type displacement gauge was attached at the position selected by visual inspection at the time of initial crack generation, and the amount of displacement after the initial crack generation was measured. Moreover, the state of cracking after the failure of the test specimens was sketched and width, direction and length of cracking was examined in detail.

4. DISCUSSION ON THE CRACKING PROPERTY OF RC SHELL ELEMENTS

(1) Load at Which Cracking Occurred

For the elucidation of the stress and deformation properties of the reinforcing bars and concrete of RC shell elements, it is important to evaluate the load at which cracking occurs realistically, and at the same time, to grasp clearly the dominant direction of cracking from the viewpoint of mechanics. The stress at which initial cracking occurred in this experiment is shown in relation to the ratio of principal loads $K=N_2/N_1$ as in Figure-2. Since the ratio of reinforcement in the RC slabs used for this experiment was relatively small, the effect that the reinforcing bars exerted on the load at which cracking occurred seemed to be negligible.

Accordingly, the main factors determining the load at which cracking occurred were considered to be the tensile strength of concrete and the ratio of in-plane principal stresses k . Since this experiment was carried out in the stress regions of uni-axial tension, compression-tension and tension-tension, first, investigation was attempted on the basis of the equation proposed by Kupfer which is frequently used as the envelope for the plain concrete strength in bi-axial stress

conditions. Kupfer expressed the equation for the strength of plain concrete in compression-tension region with Equation (1), based on the experimental results as shown in Figure 3.

$$\sigma/\sigma_{tu} = 1 + 0.8\sigma_2/\sigma_{cu} \dots\dots\dots(1)$$

Here, σ_1 : principal tensile stress when cracking occurred
(negative),

σ_2 : principal compressive stress when cracking occurred
(positive),

σ_{cu}, σ_{tu} : compressive and tensile strength of concrete.

On the other hand, the test specimens in compression-tension region in this experiment were only two, and there were not enough data to be able to confirm the criteria for the strength, but as shown in Figure-3 with marks , the values close to the equation proposed by Kupfer⁸⁾ were obtained in this experiment. Judging from this fact, it seemed non-controversial to apply the equation of Kupfer to the compression-tension region.

In the case of bi-axial tension, Kupfer assumed that failure occurs at the time when one of the bi-axial tensile stresses has reached the tensile strength of concrete, and he did not take the lowering of strength in the bi-axial tension region into account, but considering that the tensile failure of concrete arises due to the internal defects of the concrete, it seems more reasonable to consider the lowering of strength under bi-axial tensile stresses as compared with uni-axial tension region. In particular, in case of the RC slabs such as the test specimens used for this experiment, in which four reinforcing bars were arranged in 10cm thickness, the effect of the loss of cross section due to reinforcing bars seemed not to be neglected. This fact was able to be presumed from the phenomenon that the cracking in the test specimens tested at K=1.0 tended to occur mostly over the reinforcing bars.

As seen in Figure-3, the tendency can be regarded as a straight line in the range of this experiment, it is considered to be practical to estimate the stress at which cracking occurs by the following equation.

$$\sigma_1/\sigma_{tu} = 1 - \gamma k \dots\dots\dots(2)$$

Here, γ : a constant determined by experiment.

Equations (1) and (2) are shown with continuous lines in the figure. Here, σ_{tu} is the tensile strength of concrete, but in this case, the empirical formula that the authors obtained by statistical evaluation, $\sigma_{tu} = 0.573 \sigma_{cu}^{2/3}$, was used. As the result, it was judged that though the criteria for the strength somewhat overestimate the experimental data as a whole, the characteristics of the cracking load were properly expressed as its tendency. As the reason why the calculation equation described above estimated the cracking load larger than the measured values, it seemed to be originated from the fact that the state of tensile stress in the concrete slabs was not uniform, accordingly, the strength-reduction factor was introduced into these equations, and Equations (1) and (2) were to be corrected as follows;

$$-1 \leq k \leq 0 \quad \sigma_1/\sigma_{tu} = a(1 + 0.8\sigma_2/\sigma_1) \dots\dots\dots(1)'$$

$$0 \leq k \leq 1 \quad \sigma_1/\sigma_{tu} = a(1 - \gamma k) \dots\dots\dots(2)'$$

α and γ are the values determined by the configurations and dimensions of test specimens, but in the range of this experiment, $\alpha=0.90$ and $\gamma=0.26$ as shown with the broken line in Figure 3.

(2) Significance of Cracking Direction

The equations for calculating the strength of the concrete slabs with the orthogonal arrangement of reinforcement proposed so far were all theoretical ones (Peter carried out experiment also), and the assumptions on cracking direction were various. However, according to the experimental results, agreement was not necessarily obtained with the cracking direction assumed in the various equations for calculating the strength and deformation of RC shell elements proposed so far, and the cracking direction also varied in considerably in wide range. Moreover, if the existence of the cracking due to drying shrinkage and the cracking occurred owing to unexpected loading condition is to be considered, it is necessary to establish the method enabling the analysis even when cracking occurred in arbitrary directions. Any way it can be said that it is very important to define cracking direction ϕ as realistically as possible for clarifying the mechanical properties of reinforced concrete slabs after cracking has occurred.

(3) Determination of the Direction of Crack Generation as observed from Experimental Results

Photo-1 shows the crack pattern of a typical test specimen after the test. As clearly seen in this photograph, there are some continuous cracks but showing the change every section of a certain length accompanying load increase and other cracks of which the direction changed largely but which did not give the dominant influence in view of the amount of cracks in the whole RC slabs. Thereupon, the cracks observed were divided into three stages, namely just after the loading at which cracking occurred, till reinforcing bars yielded for the first time, and up to the time of failure and the relation of each cracking direction and the length as the proportion to the total crack length in each stage was examined statistically. The representative results among these are shown in Figure-4. In the figure, the abscissa shows the angle that crack direction makes with y reinforcing bars. Also, the histograms on right side show the cracking direction up to the yield load and ultimate load and the proportion of the length. Since the cracking direction was measured by the angle from y reinforcing bars, it took different values according to the declination α of reinforcing bars and the direction of principal tension. Having evaluated the direction of crack generation and the length in relation to respective α and k for all test specimens, the following remarks can be said.

i) As for the direction in which initial cracking occurred, when the value of k was zero or negative, it occurred perpendicularly to principal tension. However, when declination α was small, and accordingly the y reinforcing bars in concrete were arranged nearly in perpendicular direction to principal tension, this position became the internal defect of concrete, and the tendency of causing cracking along that defective part was also observed.

ii) On the other hand, when the value of k became as large as nearly 1.0, the stress condition close to uniform tension arose in every direction in the test specimens, consequently, regardless of the value of declination α , the cases that cracking occurred along reinforcing bars, which are the internal defective parts

as unreinforced concrete, became frequent.

iii) When k was about 0.5, it may be considered that initial cracking across perpendicularly to principal tension. After initial cracking has occurred, reinforcing bars did not yield immediately if the ratio of reinforcement was large in some extent, for instance more than 1%, the redistribution of stress occurred owing to the shearing force in the cracked surface, and the direction of initial cracking changed, or cracking occurred in different new direction. However, from the results of experiment, the amount of cracking in the direction perpendicular to principal tension ($\phi = \alpha$) increased even when load was increased, and the redistribution of stress seemed to be arising, and the cracking in the direction in which shearing force became zero at the time of yield load or failure load was not necessarily likely to be the dominant direction of cracking in RC slabs.

iv) When cracking existed in the direction of $\phi = \alpha$ before loading, the redistribution of stress occurred from the initial stage of loading, and generation of new cracks thereafter arose also in other direction than $\phi = \alpha$, but its amount was small as a whole, therefore from the direction of cracking and its length, $\phi = \alpha$ seemed to be the dominant direction of cracking. When initial cracking existed around $\phi = 50^\circ$ and its amount was small, it may be considered that existence of the initial cracking introduced beforehand did not give the dominant effect to the generation of cracks thereafter, irrespective of the value of k .

Based on the experimental results described above, the dominant direction of cracking when subjected to bi-axial loading was the direction perpendicular to principal tension, namely the direction of $\phi = \alpha$, when the value of k was negative or zero as shown in Figure-5, and when the value of k was 1.0, it was $\phi = 45^\circ$ and between those, it was assumed to be able to approximate with straight lines for convenience sake.

5. METHOD OF CALCULATING STRESS IN RC SHELL ELEMENTS BEFORE THE YIELD OF REINFORCING BARS

(1) Derivation of Equation for Calculating Stress

When the load of uni-axial or bi-axial tension or tension-compression acts at the boundary of the RC shell elements with orthogonal arrangement of reinforcement, cracking occurs perpendicularly to principal tension initially, but the redistribution of stress took place accompanying the increase of stress, and in some cases, cracking in other direction than that perpendicular to principal tension. In the case like this, from the condition of the equilibrium of force on a plane of crack making angle ϕ to reinforcing bars, the following equations hold.

$$\left. \begin{aligned} Z_x &= N_1 \cos^2 \alpha (1 + \tan \alpha \cdot \tan \phi) + N_2 \sin^2 \alpha (1 - \cot \alpha \cdot \tan \phi) + H \tan \phi \\ Z_y &= N_1 \sin^2 \alpha (1 + \cot \alpha \cdot \cot \phi) + N_2 \cos^2 \alpha (1 - \tan \alpha \cdot \cot \phi) - N \cot \phi \\ D_b &= (N_1 - N_2) \sin 2\alpha / \sin 2\phi - 2H \cot 2\phi \end{aligned} \right\} \dots\dots\dots (3)$$

Here, H is the shearing force transmitted along a cracked surface, and is given by the following equation.

$$\begin{aligned} H &= N_1 [\lambda \cot \phi \{\sin^2 \alpha (1 + \cot \alpha \cdot \cot \phi) + k \cos^2 \alpha (1 - \tan \alpha \cdot \cot \phi)\} - \tan \phi \{\cos^2 \alpha (1 + \tan \alpha \cdot \tan \phi) \\ &\quad + k \sin^2 \alpha (1 - \cot \alpha \cdot \tan \phi)\} - \nu \cdot 2 \cot (2\phi) \{(1 - k) \sin 2\alpha / \sin 2\phi\}] : [\tan^2 \phi + \lambda \cot^2 \phi \\ &\quad + \nu \cdot 4 \cot^2 (2\phi) + \xi] \dots\dots\dots (4) \end{aligned}$$

Here, Z_x, Z_y : tension of reinforcing bar groups (x) and (y).

N_1, N_2 : principal tensions acting on a reinforced concrete slab element to be studied (tension is positive) $N_1 \leq N_2, N_1 > 0, N_2 \geq 0$

D : compressive force acting in parallel with cracks in concrete

H : shearing force resisted by concrete, which should be transmitted through cracks by the interlocking of crack edges and the dowel effect of reinforcing bars crossing cracks

α : angle between the directions of principal tension N and x rein
forcement group

ϕ : angle between the directions of y reinforcement group and cracking

f_x, f_y : cross-sectional area of reinforcement groups (x) and (y)

$$\lambda = f_x / f_y, \quad \nu = f_x \cdot E_c / d \cdot E_b, \quad \xi = f_x E_c / d \cdot E_v$$

E_b, E_c : elastic modulus of concrete and reinforcing bars

First, it was assumed that the shearing deformation of the concrete between cracks was negligible, and shearing deformation in cracking direction was given by the shearing force acting on a cracked surface and the slip caused by it. In the specifically conducted push-off test of the RC blocks using orthogonal reinforcement and parallel reinforcement, loading was made by keeping crack width constant, and the relation between shearing force and slip was determined with respect to crack widths. Assuming that this relation holds in the section of one crack spacing, the shearing rigidity was evaluated (analytically, correspond to mean crack spacing).

From the result obtained in the loading test with constant crack width, the relation between the ratio of shearing stress required for displacing by unit length [hereinafter, referred to as interface shear transfer (IST) rigidity] and crack width is shown as in Figure 6, and it can be seen that irrespective of the method of reinforcement arrangement and reinforcement ratio, the shearing rigidity was expressed as the function of only crack width, with considerably good correlation.

In the figure, for the case of the compressive strength of concrete 232 kg/cm^2 (22.7 MPa) (the mean value of the strength of concrete used for this experiment), the empirical formulas of Houde,⁹⁾ Fenwick¹¹⁾ and Loeber^{12),13)} are also plotted, but the result of the authors' experiment in the range of small crack width showed the intermediate value of these three. In the range of large crack width, somewhat larger values are estimated by the authors. Generally, it is considered that the compressive strength of concrete, the kinds of aggregate, the shapes and dimensions and so on exert influence on this IST rigidity, but here, it was considered to be the function of crack width only, and to be expressed by the following empirical formula.

$$K_{IST} = \frac{36}{w} \dots \dots \dots (5)$$

Here, K_{IST} : IST rigidity ($\text{kg/cm}^2/\text{cm}$)

w : crack width (cm)

Next, the mean crack spacings of RC slabs are denoted by a_m , and as mentioned before, the shearing deformation of concrete was neglected, then denoting the shearing stress acting on a cracked surface by τ , and the relative slip by Δ , the mean shearing rigidity in cracking direction E_v can be expressed by Equation (6).

$$E_v = \frac{\tau}{\Delta} \cdot a_m \dots \dots \dots (6)$$

τ/Δ in the above equation corresponds to K_{IST} in Equation (5). In this way, the shearing rigidity E_v can be obtained by the function of crack width only (a_m becomes a constant value when the state of reinforcement arrangement is determined), but before that, the crack width of a RC slab must be determined. Namely, as clarified by many experimental results so far, the crack widths at a certain loading condition had considerable wide range of scatter even if the cracking has been in the same direction.

Therefore, in order to evaluate the behaviors of RC slabs as a whole, mean crack width must be used. When the tensile deformation of concrete is neglected, the mean crack width can be calculated by the following equation as the product of mean crack spacing a_m and the mean strain in the direction perpendicular to cracking $\epsilon_{\phi m}$.

$$W_m = a_m \epsilon_{\phi m} \dots\dots\dots(7)$$

Here, W_m : mean crack width
 a_m : mean crack spacing
 $\epsilon_{\phi m}$: mean strain in direction perpendicular to cracked surface

The mean strain used here is to be calculated by Equation (12) in the next section. Also, when the strain of x and y reinforcing bars on a cracked surface are denoted by ϵ_x and ϵ_y , respectively, from the condition of compatibility of strains on the cracked surface, the strain in the direction perpendicular to the cracked surface can be expressed by Equation (8), accordingly, also in the case of mean strain, it was assumed that Equation (9) is to hold.

$$\epsilon_{\phi} = \epsilon_x + \epsilon_y \dots\dots\dots(8)$$

$$\epsilon_{\phi m} = \epsilon_{xm} + \epsilon_{ym} \dots\dots\dots(9)$$

Here, ϵ_{ϕ} , $\epsilon_{\phi m}$: strain on a cracked surface and mean strain in the direction perpendicular to the cracked surface
 ϵ_x , ϵ_{xm} : strain at the position of crack and mean strain of reinforcing bars in x direction
 ϵ_y , ϵ_{ym} : strain at the position of crack and mean strain of reinforcing bars in y direction

On the other hand, the direction of cracking was assumed to be ϕ , and Equation (3) was rewritten, then the following Equation (10) was obtained.

$$Z_x + Z_y = (N_1 + N_2) + (N_1 - N_2) \sin \alpha \cdot \cos \alpha \cdot (\tan \phi + \cot \phi) + H(\tan \phi - \cot \phi) \dots\dots\dots(10)$$

Using Equation (4) and Equations (5) ~ (10) mentioned above, the shearing force H satisfying Equation (4) can be determined by carrying out convergence calculation for an arbitrary cracking direction ϕ and load N_1 and N_2 . However, as for a_m , the mean crack spacing determined from the condition of respective test specimens are to be used.

(2) Relation between Analyzed Values according to the Equations Proposed by the Authors and Calculations Used So Far

Based on the various conditions of in-plane loading experiment and the load at which cracking occurred for RC slabs, by applying the calculation procedure in section 5 (1), the forces in x and y reinforcing bars on a cracked surface (Z_x , Z_y) can be determined for each condition, respectively. Some examples of the representative calculation results are shown in Figure-7. In this figure, the calculated values of the forces in x and y reinforcing bars according to respective calculation equations are shown simultaneously. (The values according to the equation of Baumann are shown with marks o, and those according to the equation of Leitz are shown with marks Δ .) The abscissa shows the angle that y reinforcing bars and a cracked surface make, and the ordinate, the ratio of the calculated values of Z_x and Z_y to principal force N_1 . The curves by the calculation method of the authors were determined by assuming the load to be 30t. The shearing rigidity evaluated by the authors is different accompanying the change of crack width due to load level, therefore, Z_x/N_1 and Z_y/N_1 depend on the load level as shown in Figure-8.

In the calculation equations of Leitz and Baumann, when the arrangement of reinforcement and working load are given, the cracking directions become the constant values of 45° and ϕ_1 , respectively. Also as clearly seen in Equations (a) and (b) in Table 1, Z_x/N_1 and Z_y/N_1 do not depend on load, but become constant values. In contrast to these, in the equations of the authors, Z_x/N_1 and Z_y/N_1 changed at respective loading steps as shown in Figure-8, and in the range which is taken up in the practical design, Z_x/N_1 hardly changed as load increased, but Z_y/N_1 tended to increase considerably.

Next, referring to Figure-7, the effect of the angle of cracking direction is investigated. According to the equations proposed by the authors, the stresses of the reinforcing bars in x and y directions can be calculated in any cracking direction, but when the range of cracking was limited to within a practical range, the force in the reinforcing bars in x direction showed almost the same values when the value of k was from 0 to about 0.5, in both cases of using the calculation equations of the past and the equations of the authors.

It may be considered that the result of calculation of the force in the reinforcing bars in x direction becomes almost the same whichever equation is used. On the contrary, as for the force in the reinforcing bars in y direction, marked difference was observed among respective calculation equations even within the range of various conditions in this experiment, the results being dependent on declination α , reinforcement ratio ρ and the ratio of principal force k. In particular, the results were found to be sensitively affected by the change of the angle of cracking direction.

In this way, the stresses in y reinforcing bars underwent the influence of load level and angle of cracking direction largely as compared with x reinforcing bars, accordingly, in order to determine the force acting on y reinforcing bars conforming to the actuality and to estimate the deformation of RC shell elements with good accuracy, the equations proposed by the authors seemed to be more rational.

6. METHOD OF CALCULATING STRAIN AND DEFORMATION OF RC SHELL ELEMENTS

(1) Mean Strain of Reinforcing Bars

When the deformation and rigidity of RC slabs after the occurrence of cracking were determined using the strain of reinforcing bars in a cracked cross section, the deformation is to be overestimated, and the rigidity is to be underestimated.

Accordingly, it is important to perform the deformation analysis on the basis of mean strain in which cracking and the contribution of concrete between cracks to the rigidity are taken into consideration. This problem is essentially related to the bond behaviors between reinforcing bars and concrete, and a number of empirical formulas and theoretical equations for determining mean strain have been proposed, but here, using the method of evaluation in accordance with the CEB Code, the contribution of concrete to the tensile rigidity was taken into consideration, and the mean strain of reinforcing bars was determined. The equations for calculating deformation and crack width were derived, and the comparative study with the measured mean strain was performed. In the CEB Code, the mean strain of the reinforcing bars arranged in an effective cross section is to be expressed by Equation (11) in the case of axial tension, considering the contribution of concrete to tension.

$$\epsilon_{sm} = \frac{\sigma_s}{E_s} \left[1 - \left(\frac{\sigma_{sr}}{\sigma_s} \right)^2 \right] \leq 0.4 \frac{\sigma_s}{E_s} \dots\dots\dots(11)$$

Here, σ_s : stress of reinforcing bars in a cracked cross section under load in consideration
 σ_{sr} : stress of reinforcing bars based on the assumption of a cracked cross section just after cracking

The mean strain of reinforcing bars in this experiment was calculated by Equation (11), but as shown in Figure-9, the strain was evaluated somewhat smaller as compared with the measured values, therefore, the reduction exponent in the above equation was changed to 3 instead of 2, and the calculation of the strain was performed by the following equation.

$$\epsilon_{sm} = \frac{\sigma_s}{E_s} \left[1 - \left(\frac{\sigma_{sr}}{\sigma_s} \right)^3 \right] \dots\dots\dots(12)$$

As the result, relatively good correspondence was obtained between the measured values and the calculated values as shown in the figure, accordingly, in the analysis hereinafter, it was decided to use equation (12).

(2) Comparison with Experimental Results

(a) On the Strain of Reinforcing Bars in x and y Directions

Several strain gauges were stuck on the reinforcing bars in x and y direction in the test specimens, respectively, but in order to avoid the effect of the irregular stress at the end regions and the biased evaluation of a part of strain, four consecutive points of the measurement on one reinforcing bar were selected around the center of a test specimen, where the stress distribution seemed to be uniform, and their mean value was used as the mean experimental value.

In Figures-10 and-11, the measured values for x and y reinforcing bars and the calculated values of Leitz, Baumann and the authors in the case of $k=0$ and $\alpha=12.5^\circ$ and 22.5° are shown.

As seen in these figures, the measured values were well evaluated in the case of the strain of x reinforcing bars as compared with y reinforcing bars as mentioned before, but only the equation of Leitz at $\alpha=22.5^\circ$ showed somewhat larger value as compared with two other calculated values and the measured values.

The tendency of the force in the direction of y reinforcing bars is different from the force in the direction of x reinforcing bars, and undergoes sensitively the influence of cracking direction ϕ . Its calculated value according to the equation of Baumann showed the largest value, and particularly in the case of small α ($\alpha=12.5^\circ$), the force was several times as large as the calculated value of the authors. Also, the value obtained by the method of Leitz was considerably larger, and became about three times as large as the calculated value of the authors. From these facts, in order to estimate the forces in x and y reinforcing bars by the same procedure, it was recognized to be rational to apply the calculation equations of the authors, in which the shear transfer on a cracked surface was considered at $\phi=\alpha$ (cracking in the direction perpendicular to principal force N_1) The figure was omitted on account of limited space, but the behaviors under other conditions are mentioned as follows.

(1) Case of $k=0.5$ and $\alpha=22.5^\circ$

When the measured values for x and y reinforcing bars and the calculated values according to respective calculation equations were compared, the force in x reinforcing bars showed almost the same as calculated by any of three methods also in this case, similarly to the case of $k=0$, and the correspondence to the measured values was relatively good. Also, the force in y reinforcing bars was different from the case of $k=0$, and the difference in the results among various analysis procedures was small, moreover, relatively good agreement with the measured values was shown. However, in the range of this experiment, the equations of Leitz and Baumann evaluated somewhat larger values, whereas the equations of the authors evaluated somewhat smaller values, and from this fact, it was presumed that the assumption of cracking angle by the interpolation with straight lines proposed before was too small.

(2) Case of Making Three Cracks beforehand Perpendicular to Principal Force N_1
Namely $\phi=\alpha=22.5^\circ$ at $k=0$

In this case, the cracking in the direction of $\phi=\alpha$ was dominant, and since the measured values on that surface showed good agreement with the calculated values, it was considered that the method of calculation of the authors represented the actual phenomena fairly well. However, as seen in Photo-2, the cracking in the other direction than $\phi=\alpha$ occurred between three cracks at 36t and later. Consequently it was recognized that as mentioned before, the strain of y reinforcing bars deviated from the calculated values though gradually in the latter half of loading, by being affected sensitively by the angle of cracking direction ϕ .

(3) Case of $k=0$, $\alpha=22.5^\circ$, reinforcement ratios in x and y directions 1.18% and 0.59%

The crack pattern is shown in Photo-3.

In this test specimen, it was supposed that the shearing force transmitted through the cracked surface in the same direction became larger as compared with other test specimens, and the phenomenon of stress redistribution appeared conspicuously. Even in such test specimen, the initial cracking arose in the direction perpendicular to principal force N_1 , but thereafter, it was confirmed that the cracking with large angle of cracking direction occurred numerously, which has not been seen in the test specimens with equal reinforcement ratios in both directions under the same condition, and the phenomenon of stress redistribution

was clearly observed. Also, as mentioned before, since the strain of x reinforcing bars was not much affected by cracking direction, whichever calculated value agreed well with the measured values. However, the force in y reinforcing bars differed from the case of the reinforcement of equal amount in both directions, and the measured values showed considerably larger values than the case in which cracking direction was $\phi = \alpha$. This seemed to be caused by the fact that the effect of stress redistribution was exerted largely as compared with the case of equal reinforcement ratio, and the dominant cracking direction in the case of unbalanced reinforcement ratio became larger as compared with dominant cracking direction in the case of equal reinforcement ratios. In this connection, when comparison was made with the calculated values in which cracking direction was 35° , and the shearing force on a cracked surface was taken into account, the experimental values were able to be evaluated more accurately than making an assumption that the direction in which shearing force did not arise in a cracked surface (ϕ , $=43.28^\circ$), and it was judged that the dominant cracking direction existed between 30° and 40° .

(b) Deformation

As for the deformation of reinforced concrete slabs after cracking occurred, Equation (13) can be applied in the RC slabs with reinforcement in two orthogonal directions from the geometric condition, based on the strains of x and y reinforcing bars at the cracked sections and the slip displacement on the cracked surfaces, neglecting the deformation of concrete in the concrete struts.

$$\left. \begin{aligned} \epsilon_\phi &= \frac{\epsilon_x}{\cos^2 \phi} + \frac{\Delta}{a_m} \tan \phi = \frac{\epsilon_y}{\sin^2 \phi} - \frac{\Delta}{a_m} \cot \phi \\ \frac{\Delta}{a_m} &= \epsilon_y \cot \phi - \epsilon_x \tan \phi \\ \epsilon_1 &= \epsilon_\phi \cos^2(\phi - \alpha) - [\sin(\phi - \alpha) \cdot \cos(\phi - \alpha)] \Delta / a_m \\ \epsilon_2 &= \epsilon_\phi \sin^2(\phi - \alpha) - [\cos(\phi - \alpha) \cdot \sin(\phi - \alpha)] \Delta / a_m \end{aligned} \right\} \dots\dots\dots (13)$$

Here, Δ : slip displacement on a cracked surface
 a_m : crack spacing
 ϵ_1, ϵ_2 : strains in the directions of principal forces N_1 and N_2
 ϵ_ϕ : strain in the direction perpendicular to cracking

In Figure-12, the comparison of measured and calculated values according to Equation (13) is shown in the form of mean strain for the displacement in the direction of principal force N_1 of No.25 test specimen. However, ϵ_x and ϵ_y were determined by the calculation method of the authors, and at the time of calculating ϵ_1 , the mean strain ϵ_{1m} in the direction of principal force N_1 was determined by using the mean strain ϵ_{xm} and ϵ_{ym} , in which the contribution of concrete to the rigidity was taken into account according to Equation (12), instead of ϵ_x and ϵ_y . Also, for the comparison, the calculated values using ϵ_{xm} and ϵ_{ym} determined by the equation of Baumann (ϕ_1) are shown together. In this case also, it is clear that the correspondence of the Baumann's to the measured values was somewhat inferior to the method of the authors.

(c) Crack Width

Table-3 shows the comparison of the mean crack width of No.26 and No.27 test specimens measured with a contact point strain meter and the calculated values of mean crack width according to Equation (7) when mean crack spacings were taken as 15cm. Except the loading stage in which the stress intensity of reinforcing bars was small and the number of cracks was not stable, the calculated values showed relatively good agreement with the experimental results. Also, when the mean crack width was plotted in relation to the sum of the stress intensity of x and y

reinforcing bars, the result is as shown in Figure-13. As expected by Equation (8), the correlation was observed between the mean crack width and the total stress intensity of reinforcing bars in a cracked cross section, regardless of the value of α .

(d) Slip Deformation on Cracked Surface

In a cracked surface in the direction along which shearing force does not arise, slip displacement Δ does not occur, but in other cracking direction than that, shearing force arise, and it is considered that slip deformation occurred due to this shearing force. In No.25 test specimen, cracking was introduced in the direction of $\phi=\alpha$ beforehand, and the slip displacement was measured by attaching a displacement gauge across that cracked surface. The result is shown in Figure-14. On the other hand, using the shearing rigidity in cracking direction E_v , the slip displacement along a cracked surface can be calculated. In the figure, two calculated values are shown, but there is not much difference between the calculated values, and the measured values were presumed accurately, accordingly, it can be said that the evaluation of the shearing rigidity along a cracked surface was appropriate.

7. METHOD OF CALCULATING STRENGTH OF RC SHELL ELEMENTS

(1) Calculation of Yield Load of Reinforcing Bars

The load at which cracking occurred, the yield load of x and y reinforcing bars and the largest load obtained by the experiment on reinforced concrete slabs are shown in Table 4 together with other properties of the test specimens.

In the previous section, when the mechanical properties of reinforced concrete slabs after cracking were examined, the mean strain of reinforcing bars was evaluated by the comparison in accordance with the ideas of three researchers, based on the measured cracking direction paying attention to the direction in which cracks occurred. In this section, the yield load of x reinforcing bars which yielded first was determined by the three methods mentioned before and compared with the measured values, thus the applicability of these equations was evaluated on a comparative basis. The principal force N_1 at the time of the yield of x reinforcing bars calculated on the basis of three methods, the measured N_1 and their ratio (measured/calculated) are shown in Table-5. Moreover, in this case, at the time of determining the yield load of x reinforcing bars, it was assumed that the bond of the reinforcing bars between cracks was completely lost. Actually, it cannot be said that this assumption is correct in the strict sense, but near the load at which reinforcing bars yielded, the dispersion of cracking seemed to advance sufficiently, and the effect of bond seemed to be lost, therefore it is considered to be permitted practically to make this assumption. As seen clearly in this table, as k changed from +1.0 toward -1.0, the calculated values of Leitz tended to underestimate the test results as compared with the measured values. As examined in 4. (3), this was caused by the fact that as k approached -1.0, the direction of crack generation ϕ approached α , and as seen in the experimental result at $k=-1.0$, ϕ did not become 45° as Leitz assumed. The coefficient of variation for the values by the methods of Baumann and the authors were 9.6% and 9.2%, respectively, while that of Leitz became 14.4%, thus the accuracy of estimation based on the measured values became inferior for Leitz. Also, in the estimation of the yield load of x reinforcing bars by the methods of Baumann and the authors, the ratio of the measured/the calculated did not depend on the value of k over the whole range of k , and it can be said that the

applicability of whichever equation was sufficient.

However as mentioned before, since the strain of x reinforcing bars was not affected sensitively by the angle of cracking direction ϕ , the phenomenon described above was observed, and it may be said that the method of the authors, by which the estimation of the strain of y reinforcing bars can be made regardless of cracking direction, is the analysis method with wide generality, which can determine the mechanical properties of reinforced concrete slabs subjected to in-plane forces conforming to the actuality.

(2) Estimation of Strength after Yield of x Reinforcing Bars

Up to the loading stage in which x reinforcing bars have yielded, the equation for estimating strength taking the shearing force on a cracked surface into account in the cracking direction changing with the value of k was employed as mentioned before, and as for the load increment after x reinforcing bars have yielded, it was considered that the increment of load carried by x reinforcing bars ΔZ_x was zero, and that resistance was put up only by the increment of load carried by y reinforcing bars ΔZ_y and the increment of shearing force component on a cracked surface ΔH , and only the balance of forces for the increment was to be considered.

Assuming cracking direction as ϕ ,

$$\Delta Z_x = 0 = N_1' \cos^2 \alpha (1 + \tan \alpha \cdot \cot \phi) + N_2' (1 - \cot \alpha \cdot \tan \phi) + \Delta H \tan \phi \quad (14)$$

$$\Delta Z_y = N_1' \sin^2 \alpha (1 + \cot \alpha \cdot \cot \phi) + N_2' \cos^2 \alpha (1 + \tan \alpha \cdot \cot \phi) - \Delta H \cot \phi \quad (15)$$

$$\begin{aligned} \text{where, } N_1' &= N_1 - N_1^{x \text{ yield}} \\ N_2' &= N_2 - N_2^{x \text{ yield}} \\ \Delta Z_y &= Z_y - Z_y^{x \text{ yield}} \end{aligned}$$

Here, $N_1^{x \text{ yield}}$, $N_2^{x \text{ yield}}$: load N_1 and N_2 when x reinforcing bars yielded
 $Z_y^{x \text{ yield}}$: load in the direction of y reinforcing bars when x reinforcing bars yielded
 N_1, N_2 : working load

ΔH was determined by Equation (14), and substituted into Equation (15), then Equation (16) was obtained.

$$\Delta Z_y = N_1' \{ \cos^2 \alpha (1 + \tan \alpha \cdot \tan \phi)^2 + k \sin^2 \alpha (1 - \tan \phi \cdot \cot \alpha)^2 \} \cdot \cot^2 \phi \quad (16)$$

$$\text{Here, } k = \frac{N_2}{N_1} = \frac{N_2'}{N_1'}$$

Accordingly, by determining N_1' and N_2' for the increment of load carried by y reinforcing bars until they have yielded ($\Delta Z_y = Z_y^{y \text{ yield}} - Z_y^{x \text{ yield}}$), the strength when y reinforcing bars have yielded can be obtained.

$$N_1^{y \text{ yield}} = N_1^{x \text{ yield}} + N_1' \quad (17)$$

Here, $N_1^{y \text{ yield}}$: load N_1 when y reinforcing bars have yielded

The yield load of y reinforcing bars in RC slabs calculated by the procedures described above is shown in Table 6 together with the experimental results. When the yield load of y reinforcing bars was not able to be measured exactly, the largest load was taken as the yield load of y reinforcing bars. The mean value of the ratios measured/calculated for all test specimens was 1.06, and the coefficient of variation was 8.2%, accordingly it is judged that the method of presuming the yield load of y reinforcing bars described above is sufficiently usable from the practical viewpoint.

8. SUMMARY

In this research, for the purpose of rationalizing the design of cross sections of reinforced concrete cylindrical shells such as the containment vessels for nuclear power stations are subjected to in-plane shearing force at the time of earthquakes in addition to in-plane membrane forces, the shell elements subjected to in-plane forces were modeled, and the loading test on the RC slabs in which reinforcement was arranged in two orthogonal directions was carried out. The experimental results were examined, and the practical method of analysis in conformity with the actual properties was proposed by revising the existing theories of analysis. The main results of this research are summarized as follows.

(1) The testing setup and the test specimens used for this research to load in-plane forces in two directions on RC slabs improved essentially such problems as the unevenness of loading and the anchoring of reinforcing bars which have been problematic in the methods used so far, and it was confirmed that they were appropriate as the testing method for RC shell elements in the range where shearing force is not predominant.

(2) The cracking strength of the RC shell elements subjected to the in-plane principal stresses in two directions can be evaluated by the equation proposed by Kupfer in the region where the stress condition is compression-tension, but in the region of tension-tension, it is necessary to reduce the cracking strength corresponding to the stress ratio. In this case, correction must be made by multiplying the cracking strength of shell elements obtained from the strength value in the material testing by the strength reduction factor.

(3) Based on the viewpoint that the cracking direction to be assumed for the analysis of the stress and deformation of RC shell elements plays an important role, the statistical analysis of the dominant cracking direction was performed for the experimental results, and the empirical formula for giving cracking direction, which is applied to the case with the equal amount of reinforcement in two directions, was determined as a function of the ratio of principal stresses.

(4) As the method of calculating the stress and deformation of RC shell elements, using the method of Baumann as the basis, the procedure of analysis was proposed in which the stress dependence of cracking direction described above, the crack width dependence of the shearing rigidity transferred through crack edges, and the contribution of the concrete portion between cracks to the tensile rigidity were

taken in consideration. It was clarified that the result of analysis by this procedure showed better agreement with the measured values than the calculated values of the stress, deformation and crack width by the procedures used so far. In particular, as for the calculation of the stress of reinforcing bars which make larger angle with the larger principal tensile stress (y reinforcing bars), it was shown that the applicability of the equations proposed by the authors was especially high.

(5) The procedure of calculating the load at which the reinforcing bars in y direction, carrying the small share of load in RC shell elements, yield, was proposed, and it was confirmed that this procedure was able to presume the yield strength of the reinforcing bars in y direction within the range of almost same coefficient of variation (about 10%) as the reinforcing bars in x direction.

ACKNOWLEDGEMENT

Heartfelt gratitude of the authors is expressed to Professor Hajime Okamura, Professor Fumio Nishino and Assistant Professor Shunsuke Kotani of the University of Tokyo, who gave kind guidance extended to them for the preparation of the present paper.

REFERENCE

- [1] Leitz, H.: Eisenbewehrte Platten bei Allgemeinen Biegunszustanden, Bautechnik, Heft 32, 1923.
- [2] Flügge, W.: Static und Dynamik der Schalen, 3rd ed., Berlin, Springer-Verlag, 1962.
- [3] Peter, J.: Zur Bewehrung von Scheiben und Schalen für Hauptspannungen Schiefwinklig zur Bewehrungsrichtung, Die Bautechnik, Vol. 43, No. 5, pp. 149-154, 1966-5, and Vol. 43, No. 7, pp. 240-248, 1966-7.
- [4] Baumann, T.: Zur Frage der Netzbewehrung von Flächentragwerken, Der Bauingenieur, Vol. 47, Heft 10, pp. 367-372, 1972.
- [5] Baumann, T.: Tragwirkung Orthogonaler Bewehrungsnetze Beliebiger Richtung in Flächentragwerken aus Stahlbeton, Deutscher Ausschuss für Stahlbeton, Heft 217, Berlin, 1972.
- [6] Duchon, N.B.: Analysis of Reinforced Concrete Membrane Subject to Tension and Shear, ACI Journal, Vol. 69, No. 9, pp. 578-583, 1972-9.
- [7] Bazant, Z.P. and T. Tsubaki: Concrete Reinforcing Net: Optimum Slip-Free Limit Design, Proc. of ASCE, Vol. 105, No. ST2, pp. 327-346, February 1979.
- [8] Kupfer, H.B., H.K. Hilsdorf and H. Rüschi: Behavior of Concrete under Biaxial Stresses, ACI Journal, Vol. 66, No. 8, pp. 656-665, 1969-8.
- [9] Houde, J.: Study of Force-Displacement Relationship for the Finite Element Analysis of Reinforced Concrete, Structural Concrete Series, No. 73-2, McGill University, Montreal, December 1973.
- [10] Mirza, M.S. and J. Houde: A Finite Element Analysis of Shear Strength of Reinforced Concrete Beams, ACI Special Publication SP 42-5, Vol. 1, "Shear in Reinforced Concrete", Detroit, Michigan, pp. 103-128, 1974.
- [11] Fenwick, R.C. and T. Paulay: Mechanisms of Shear Resistance of Concrete Beams, Journal of Structural Division, ASCE, Vol. 94, No. ST10, Proc. Paper 2325, pp. 2325-2350, October 1968.
- [12] Loeber, P.J.: Shear Transfer by Aggregate Interlock, M.E. Thesis, University of Canterbury, Christchurch, New Zealand, 1970.

[13] Paulay, T. and P.J. Loeber: Shear Transfer by Aggregate Interlock, ACI Special Publication SP 42-1, Shear Transfer in Reinforced Concrete, Vol. 1, Detroit, Michigan, pp. 1~15, 1974.

Table—1 Calculating equations concerning reinforced concrete shell elements with orthogonal arrangement of reinforcement

Proposer	Proposed equation
Leitz ¹⁾ (a)	$Z_x = N_1 \cos^2 \alpha + N_2 \sin^2 \alpha + (N_1 - N_2) \sin \alpha \cdot \cos \alpha$ $Z_y = N_1 \sin^2 \alpha + N_2 \cos^2 \alpha + (N_1 - N_2) \sin \alpha \cdot \cos \alpha$ $D_b = 2(N_1 - N_2) \sin \alpha \cdot \cos \alpha$
Flügge ²⁾ (b)	$Z_x = N_1 \cos^2 \alpha + N_2 \sin^2 \alpha$ $Z_y = N_1 \sin^2 \alpha + N_2 \cos^2 \alpha$ $D_b = (N_1 - N_2) \sin \alpha \cdot \cos \alpha$
Peter ³⁾ (c)	<p>i) When the lateral movement of wall parts formed by cracking is free $Z_x = Z_y = D_b = N_1$, $H = 0$</p> <p>ii) When the lateral movement of wall parts formed by cracking is completely constrained</p> $Z_x = N_1 \frac{\cos \alpha}{\cos^2 \alpha + \frac{\sigma_y}{\sigma_x} \lambda \sin^2 \alpha}$ $Z_y = N_1 \frac{\sin \alpha}{\sin^2 \alpha + \frac{\sigma_x}{\sigma_y} \frac{1}{\lambda} \cos^2 \alpha}$ $H = Z_x \sin \alpha - Z_y \cos \alpha$ <p>σ_x, σ_y : stress of x and y reinforcing bars $\lambda = \frac{f_y}{f_x}$ f_x, f_y : cross section of reinforcing bars per unit width in x and y directions $\frac{\epsilon_y}{\epsilon_x} = \frac{\sigma_y}{\sigma_x} = \tan^2 \alpha$</p>
Baumann ^{4),5)} (d)	$Z_x = N_1 \cos^2 \alpha (1 + \tan \alpha \cdot \tan \varphi_1) + N_2 \sin^2 \alpha (1 - \cot \alpha \cdot \tan \varphi_1)$ $Z_y = N_1 \sin^2 \alpha (1 + \cot \alpha \cdot \cot \varphi_1) + N_2 \cos^2 \alpha (1 - \tan \alpha \cdot \cot \varphi_1)$ $D_b = (N_1 - N_2) \sin 2 \alpha / \sin 2 \varphi_1$ <p>φ_1 is the value satisfying the following equation.</p> $\cot^4 \varphi_1 + \cot^3 \varphi_1 \frac{\tan \alpha + K \cot \alpha}{1 - K} - \cot \varphi_1 \frac{\cot \alpha + K \tan \alpha}{\lambda (1 - K)} - \frac{1}{\lambda} = \frac{\nu}{\lambda} (1 - \cot^4 \varphi_1)$ <p>$\lambda = f_x / f_y$ (the ratio of reinforcing bar areas in x and y direction) $\nu = \mu_x E_c / E_b$ μ_x : reinforcement ratio in x direction E_c, E_b : elastic moduli of reinforcing bars and concrete</p>
Düchon ⁶⁾ (e)	$\sigma_x = (\epsilon_1 \sin^2 \beta + \epsilon_2 \cos^2 \beta) E_s$ $\sigma_y = (\epsilon_1 \cos^2 \beta + \epsilon_2 \sin^2 \beta) E_s$ $\sigma_c = \epsilon_2 \cdot E_c$ $\gamma = (\epsilon_1 - \epsilon_2) \sin^2 \beta$ <p>ϵ_1, ϵ_2 : principal strain σ_x, σ_y : stresses of x and y reinforcing bars E_s, E_c : elastic moduli of reinforcing bars and concrete σ_c : compressive stress of concrete γ : shearing strain</p>
Bazzant ⁷⁾ Tsubaki (f)	$(N_x)_{\text{opt}} = 1 + \frac{1}{2} (1 - m) \sin 2 \alpha (\operatorname{cosec} \beta - \tan \alpha)$ $(N_y)_{\text{opt}} = m + \frac{1}{2} (1 - m) \sin 2 \alpha (\operatorname{cosec} \beta + \tan \alpha)$ <p>β : $\tan^{-1}(k)$ m : N_2 / N_1 n_x : N_x^* / N_1 n_y : N_y^* / N_1 N_x^*, N_y^* : product of amount of reinforcing bars and yield stress of reinforcing bars in x and y directions k : coefficient of friction on cracked surface</p>

Table 2 Mix. proportion of concrete and strength properties of reinforcing bars used for experiment

Mix proportion

Water cement ratio (%)	Ratio of fine aggregate (%)	Slump (cm)	Air content (%)	Unit content (kg/m³)					
				Water	Cement	Fine aggregate	Coarse aggregate		Pczzolith No.51
							10~20mm	5~10mm	
77	52	10±1	3±1	179	332	966	626	313	0.580

Strength properties of reinforcing bars
(kg/cm² = 0.098MPa)

	Yield point σ_y (kg/cm ²)	Average	Tensile strength σ_k (kg/cm ²)	Average
D ϕ 6	3,790	3,790	5,665	5,711
	3,790		5,722	
	3,790		5,747	
D ϕ 10	3,813	3,785	5,482	5,510
	3,841		5,524	
	3,701		5,524	

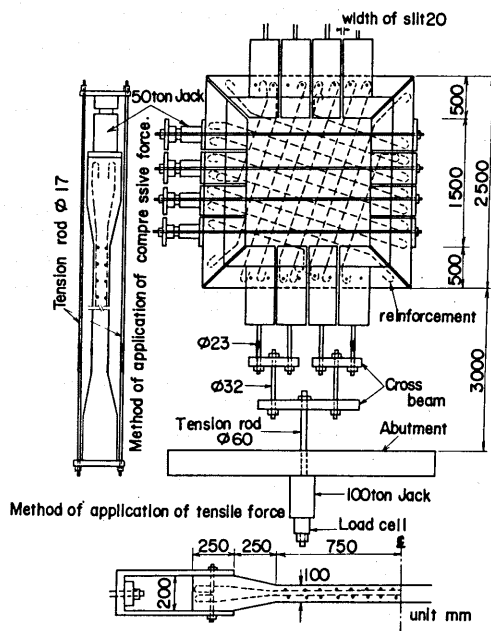


Figure 1 Shape and dimension of a test specimen

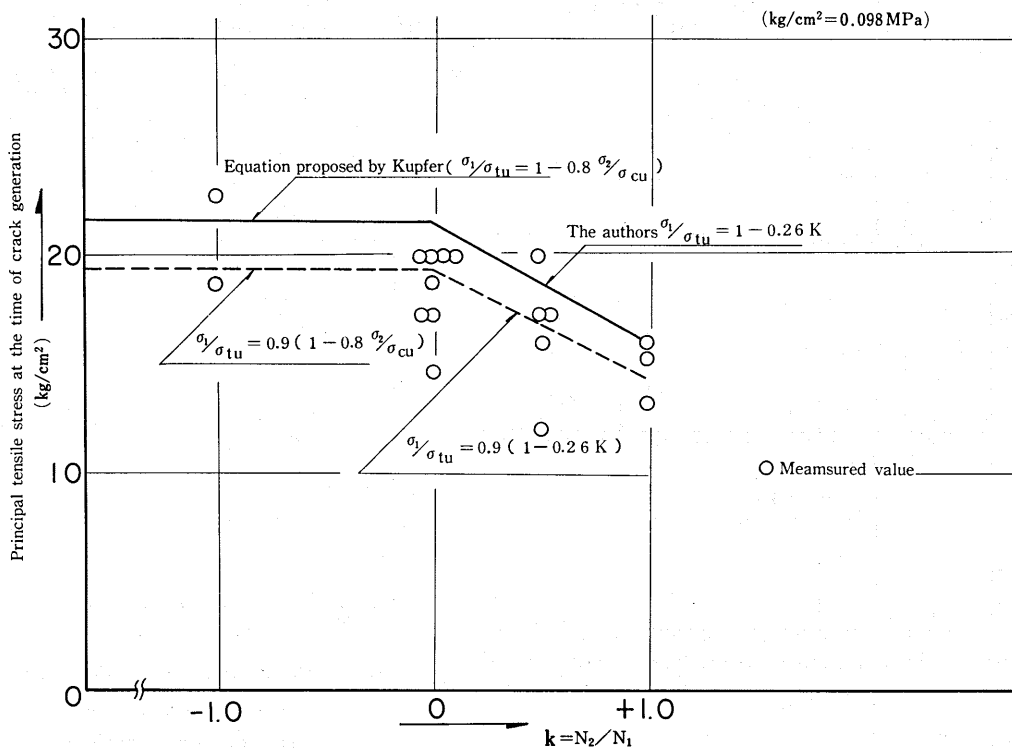


Figure 2 Relation between principal tensile stress ratio (N_x/N_1) and principal tensile stress intensity (σ_1) at the time of cracking

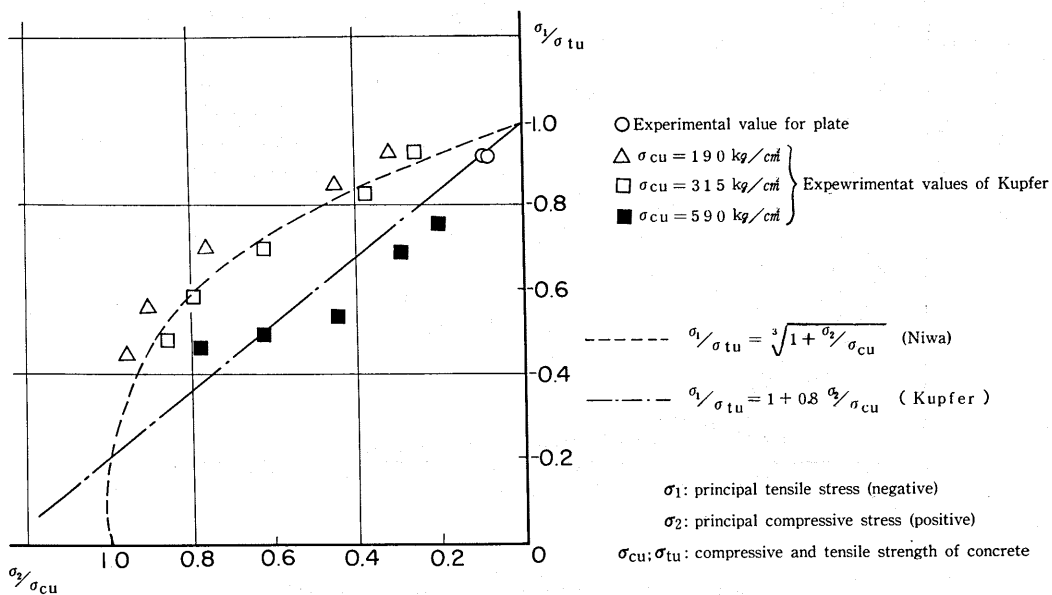


Figure 3 Strength criteria in compression-tension region

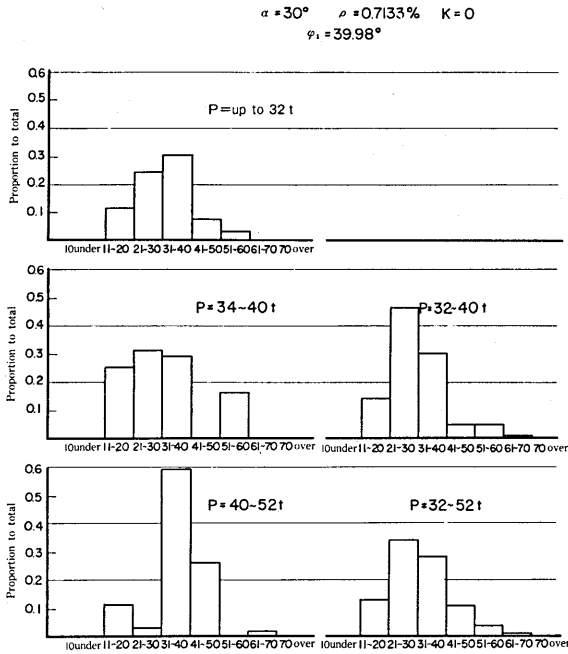


Figure 4 Distribution of occurrence frequency of cracking angle in No.15 test specimen

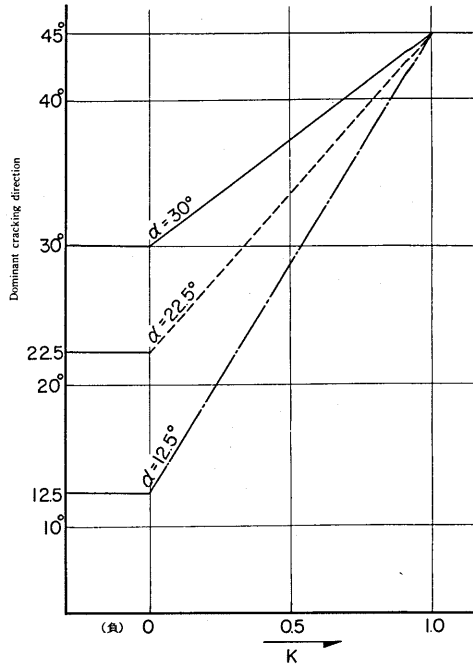


Figure 5 Relation between dominant cracking direction and principal force ratio k

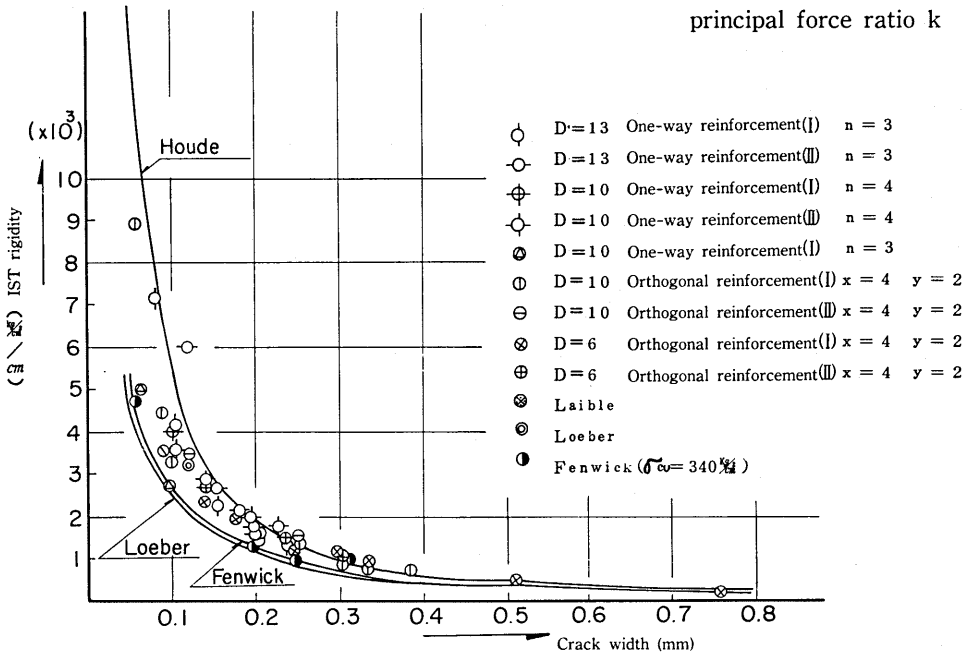


Figure 6 Relation between crack width and IST rigidity in Push-off test specimens ($1 \text{ kg/cm}^2 = 0.098 \text{ MPa}$)

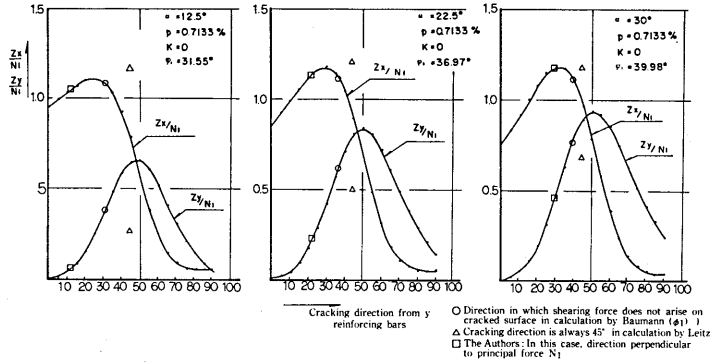


Figure 7 Relation between cracking direction and calculated values of Zx/N_1 and Zy/N_1

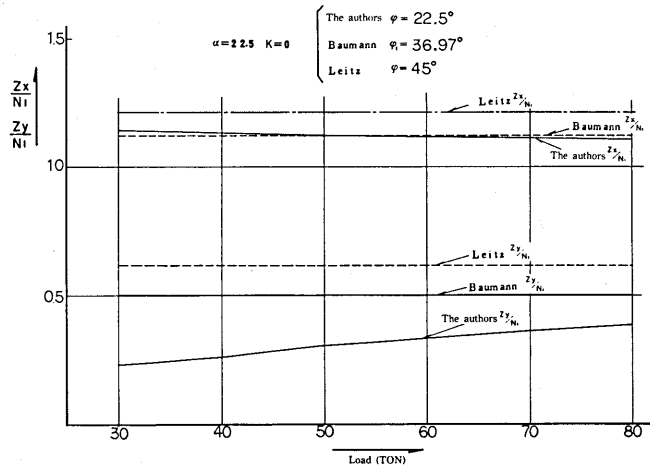


Figure 8 Relation between Zx/N_1 , Zy/N_1 and load according to respective calculation equations

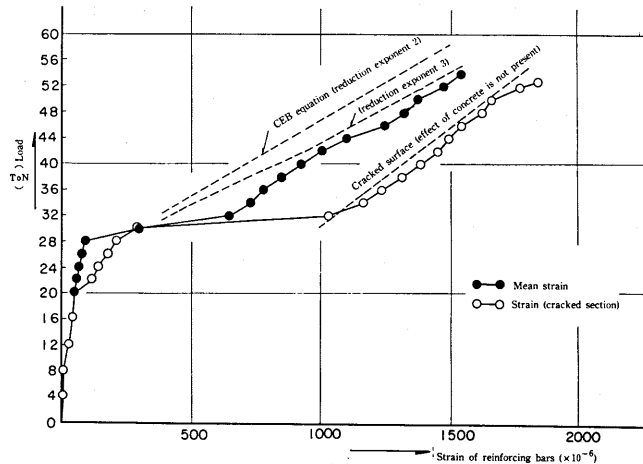


Figure 9 Measured values and calculated values of mean strain and largest strain of X reinforcing bars in No.23 test specimen

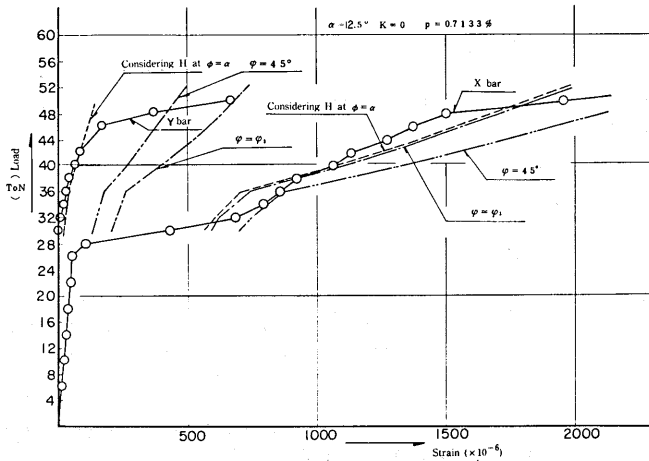


Figure 10 Measured values and calculated values of mean strain of x and y reinforcing bars in No.11 test specimen

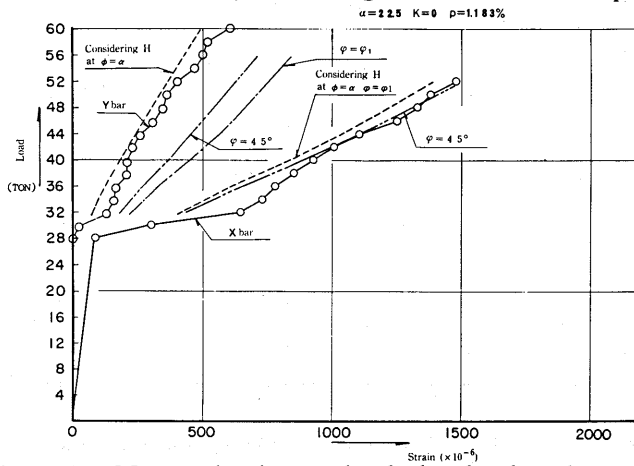


Figure 11 Measured values and calculated values for strain of x and y reinforcing bars in No.23 test specimen

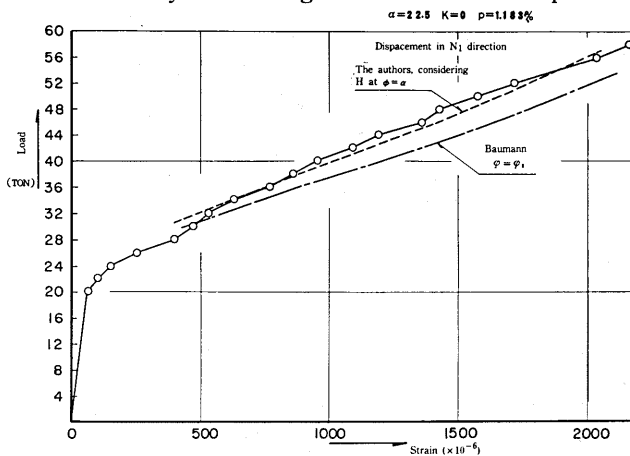


Figure 12 Comparison of measured and calculated values of mean strain in N_1 direction in No.25 test specimen

Table 3 Comparison of measured values and calculated values of mean crack widths

No. 26 test specimen				No. 27 test specimen			
Load	Measured mean crack width (mm)	Calculated values		Load	Measured mean crack width (mm)	Calculated values	
		Crack width (mm)	Measured/Calculated			Crack width (mm)	Measured/Calculated
30	0.085	0.101	0.842	26	0.092	0.075	1.267
34	0.159	0.115	1.383	30	0.096	0.087	1.103
38	0.189	0.163	1.160	34	0.174	0.136	1.280
42	0.232	0.226	1.027	38	0.184	0.187	0.984
46	0.258	0.281	0.918	42	0.200	0.232	0.862
50	0.289	0.331	0.873	46	0.241	0.273	0.883
54	0.330	0.378	0.873	50	0.280	0.311	0.900
58	0.370	0.422	0.837	54	0.321	0.348	0.922
62	0.384	0.465	0.826	58	0.379	0.382	0.992
Mean value		0.971		Mean value		1.021	
Variation factor		18.3%		Variation factor		14.8%	

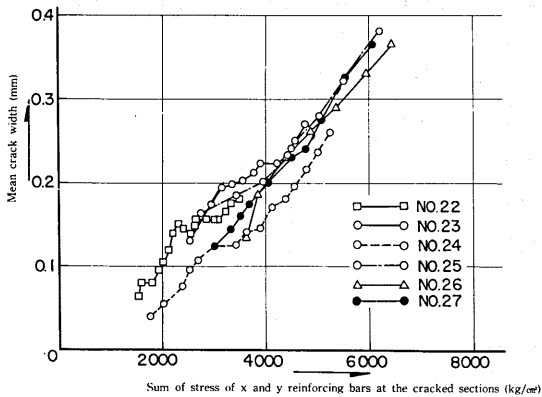


Figure 13 Relation between sum of stresses of reinforcing bars at cracked sections in both directions and mean crack widths

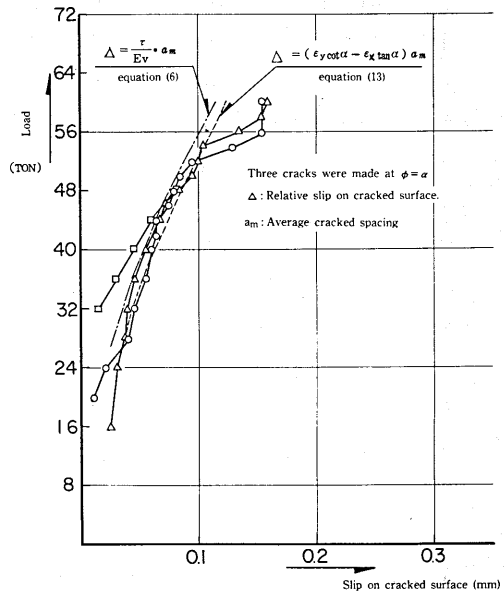


Figure 14 Measured values and calculated values of relative slip on cracked surface in No.25 test specimen

Table 4 Test results of reinforced concrete slabs

(kg/cm² = 0.098MPa)

Test specimen No.	Particulars of test specimens				Test result						
	Reinforcement ratio p (%)	Declination of principal force to x bare α	Presence of initial cracking (°)	$K = \frac{N_2}{N_1}$	Properties of concrete			The kings of loads (t)			
					σ_{cu} (Kg/cm ²)	σ_{tu} (Kg/cm ²)	E_c ($\times 10^5$ Kg/cm ²)	Initial cracking load	x reinforcing bars	y reinforcing bars	Ultimate load
20	0.761	0	None	0	201	20.6	2.10	26.0	44.0		63.5
6	0.761	0	None	0.5	249	22.0	2.35	30.0	40.0		64.0
11	0.713	12.5	None	0	207	23.2	2.20	30.0	44.0		56.0
12	0.713	12.5	None	1.0	253	25.5	2.58	23.0	38.0	42.0	46.0
7	0.713	22.5	None	0	239	21.5	2.34	30.0	36.0	44.0	50.0
8	0.713	22.5	None	0.5	251	20.3	2.35	26.0	36.0	41.0	48.0
9	0.713	22.5	None	1.0	262	24.4	2.70	20.0	36.0		44.0
13	0.713	22.5	None	-1.0	215	22.8	2.44	28.0	38.0		46.0
15	0.713	30.	None	0	225	23.7	2.12	26.0	38.0	48.5	52.0
2	0.713	30	None	0.5	254	21.3	2.51	24.0	34.0	48.0	52.0
4	0.713	30	None	1.0	278	23.7	2.75	24.0	36.0	38.5	52.0
19	0.713	45	None	0.5	181	20.8	1.90	18.0	44.5	49.0	49.0
21	0.713	45	None	-1.0	284	24.0	2.45	34.0	42.0		51.5
3	0.713	30	30	0	282	27.2	2.74	—	33.5	40.0	48.0
17	0.713	30	57	0.5	219	22.8	1.93	—	47.5	47.0	56.0
10	0.713	22.5	22.5	0.5	207	21.5	2.17	—	34.5	40.5	44.0
14	0.713	22.5	22.5	-1.0	222	20.8	2.20	—	34.0		50.0
16	0.713	22.5	49	-1.0	208	22.4	2.00	—	39.5		49.0
22	1.183	0	None	0	246	22.0	2.15	30.0	66.0		92.0
23	1.183	22.5	None	0	202	19.0	2.11	28.0	53.0		79.0
27	1.183	22.5	None	0.5	211	19.3	2.09	26.0	60.0	64.0	87.5
25	1.183	22.5	22.5	0	221	21.2	2.07	—	51.0		82.5
26	1.183	45	None	0	204	21.3	2.21	30.0	61.5	69.0	82.0
24	x: 1.183 y: 0.592	22.5	None	0	217	21.6	2.17	22.0	51.0	58.5	65.0

Table 5 Yield load of x reinforcing bars

Test specimen No.	Particulars of test specimens				N_1 x yield	N_1 max	Leitz		Baumann		The authors	
	p	α	Presence of cracking	$K = \frac{N_2}{N_1}$			N_1^{cal} x yield	Measured /calculated	N_1^{cal} x yield	Measured /calculated	N_1^{cal} x yield	Measured /calculated
20	0.761	0	None	0	44.0	63.5	43.2	1.02	43.2	1.02	43.2	1.02
6	0.761	0	None	0.5	40.0	64.0	43.2	0.93	43.2	0.93	43.2	0.93
11	0.713	12.5	None	0	44.0	56.0	35.7	1.23	37.2	1.18	38.6	1.14
12	0.713	12.5	None	1.0	38.0	46.0	40.5	0.94	40.5	0.94	40.5	0.94
7	0.713	22.5	None	0	36.0	50.0	33.5	1.07	36.1	1.00	35.6	1.01
8	0.713	22.5	None	0.5	36.0	48.0	36.7	0.98	37.4	0.96	35.0	1.03
9	0.713	22.5	None	1.0	36.0	44.0	40.5	0.89	40.5	0.89	40.5	0.89
13	0.713	22.5	None	-1.0	38.0	46.0	28.6	1.33	35.0	1.09	35.5	1.07
15	0.713	30	None	0	38.0	52.0	34.2	1.11	36.3	1.05	34.4	1.10
2	0.713	30	None	0.5	34.0	52.0	37.1	0.92	37.8	0.90	37.6	0.90
4	0.713	30	None	1.0	36.0	52.0	40.5	0.89	40.5	0.89	40.5	0.89
19	0.713	45	None	0.5	44.5	49.0	40.5	1.10	40.5	1.10	40.5	1.10
21	0.713	45	None	-1.0	42.0	51.5	40.5	1.04	40.5	1.04	40.5	1.04
3	0.713	30	$\phi=30$	0	33.5	48.0	34.2	0.99	36.3	0.92	34.4	0.97
17	0.713	30	$\phi=57$	0.5	47.5	56.0	37.1	1.28	37.8	1.26	37.6	1.26
10	0.713	22.5	$\phi=22.5$	0.5	34.5	44.0	36.7	0.94	37.4	0.92	35.0	0.99
14	0.713	22.5	$\phi=22.5$	-1.0	34.0	50.0	28.6	1.19	35.0	0.97	35.5	0.96
16	0.713	22.5	$\phi=49$	-1.0	39.5	49.0	28.6	1.38	35.0	1.13	35.5	1.11
22	1.183	0	None	0	66.0	92.0	67.2	0.98	67.2	0.98	67.2	0.98
23	1.183	22.5	None	0	53.0	79.0	55.6	0.95	56.8	0.93	57.1	0.93
27	1.183	22.5	None	0.5	60.0	87.5	60.9	0.99	59.1	1.02	56.4	1.06
25	1.183	22.5	$\phi=22.5$	0	51.0	65.0	55.6	0.92	56.8	0.90	57.1	0.89
26	1.183	45	None	0	61.5	82.0	67.2	0.92	67.2	0.92	67.2	0.92
24	$x=1.183$ $y=0.592$	22.5	None	0	51.0	65.0	55.6	0.92	52.5	0.97	54.2	0.94
Average								1.04	1.00		1.00	
Coefficient of variation								14.4%	9.6%		9.2%	

Table 6 Yield load of y reinforcing bars

(t)

Test specimen No.	Particulars of test specimen			Angle of cracking direction (°)	Yield load of y reinforcing bars		
	Reinforcement ratio p (%)	α	$K = N_2/N_1$		Experimental value	Calculated value	Measured/Calculated
12	0.713	12.5	1.0	45	42.0	40.5	1.04
7	0.713	22.5	0	22.5	44.0	40.5	1.09
8	0.713	22.5	0.5	33.8	41.0	41.3	0.99
15	0.713	30	0	30	48.5	40.5	1.20
2	0.713	30	0.5	37.5	48.0	42.8	1.12
4	0.713	30	1.0	45	38.5	40.5	0.95
19	0.713	45	0.5	45	49.0	40.5	1.21
3	0.713	30	0	30	40.0	40.5	0.99
17	0.713	30	0.5	37.5	47.0	40.9	1.15
10	0.713	22.5	0.5	33.8	40.5	41.3	0.98
27	1.183	22.5	0.5	33.8	64.0	65.6	0.98
26	1.183	45	0	45	69.0	67.2	1.03
24	X = 1.183 Y = 0.592	22.5	0	22.5	58.5	57.0	1.02
Mean value							1.06
Variation factor							8.2%

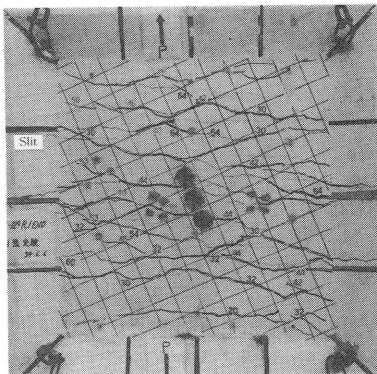


Photo. 1 No.23 test specimen
(uniaxial tension test)

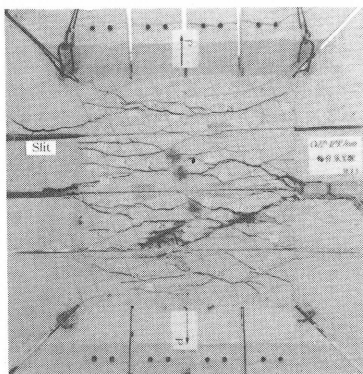


Photo. 2 No.25 test specimen
(three cracks were made at $\phi = \alpha$)

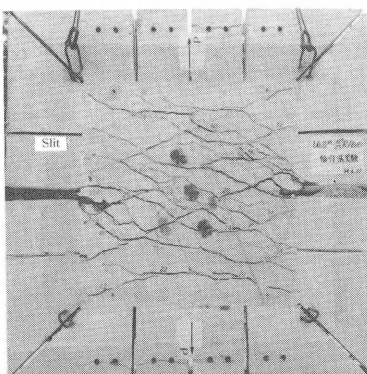


Photo. 3 No.24 test specimen